LPTENS-95/24

in memoriam Claude Itzykson

Almost Flat Planar Diagrams

Vladimir A. Kazakov
Matthias Staudacher †
and
Thomas Wynter †

Laboratoire de Physique Théorique de
l'École Normale Supérieure *

We continue our study of matrix models of dually weighted graphs. Among the attractive features of these models is the possibility to interpolate between ensembles of regular and random two-dimensional lattices, relevant for the study of the crossover from two-dimensional flat space to two-dimensional quantum gravity. We further develop the formalism of large N character expansions. In particular, a general method for determining the large N limit of a character is derived. This method, aside from being potentially useful for a far greater class of problems, allows us to exactly solve the matrix models of dually weighted graphs, reducing them to a well-posed Cauchy-Riemann problem. The power of the method is illustrated by explicitly solving a new model in which only positive curvature defects are permitted on the surface, an arbitrary amount of negative curvature being introduced at a single insertion.

June 1995

† This work is supported by funds provided by the European Community, Human Capital and Mobility Programme.

* Unité Propre du Centre National de la Recherche Scientifique, associée à l'École Normale Supérieure et à l'Université de Paris-Sud.

1. Introduction

Hermitian one matrix models were introduced and for the first time solved in the large N limit in the seminal paper by Brézin, Itzykson, Parisi and Zuber [1]. These models generate ensembles of planar, random graphs whose vertex coordination numbers are controlled by the matrix potential. By varying the potential, different classes of diagrams may be obtained, e.g. random square or random triangular lattices. However, despite this freedom, there is a class of physically important lattices that can not be generated by simply tuning the potential: *regular*, flat lattices with fixed coordination numbers of both vertices and faces. To attain them it is necessary to study planar graphs having coordination number dependent weights for both the vertices and faces. It is straightforward to define modified hermitian matrix models producing such graphs, but they can no longer be treated with the methods of [1]. In fact, until very recently this class of models of dually weighted graphs seemed intractable. However, an important but little noticed observation due to Itzykson and Di Francesco [2] has made possible the explicit treatment of dually weighted graphs. The number of degrees of freedom of these models is crucially reduced by rewriting the model in the language of group theory. It should also be noted that this method, based on expanding the matrix model potential in Weyl characters, was already used presciently in a special case in another early paper by Itzykson and Zuber [3]. In a recent work [4] we demonstrated that this new approach leads indeed to a problem amenable to mathematical analysis once the large N limit is taken.

The physical importance of matrix models has been elucidated through a large body of work over the last ten years. In [5] [6] matrix models were first introduced to furnish a description of two-dimensional quantum gravity and non-critical bosonic strings and successfully used to calculate the critical properties of these theories. This approach is based on the representation of the sum over world-sheet metrics as a sum over dynamical triangulations as originally proposed in [5] [6] [7]. Studying the crossover from random, dynamical graphs to regular, static graphs, then, will correspond to suppressing the curvature fluctuations of the world-sheet metric and result in a flat two-dimensional metric. Our work, in conjunction with [4], should thus be seen as representing a first attempt towards establishing a connection between integrable two-dimensional models both coupled to and decoupled from quantum gravity.

To be precise, let us consider general planar graphs and introduce a set of couplings $t_1^*, t_2^*, ...t_q^*, ...$, namely the weights of vertices with $1, 2, ..., q, ...$ neighbours, and a dual set $t_1, t_2, ...t_q, ...$, the weights of the dual vertices (or faces) with appropriate coordination numbers. The partition function of closed planar graphs G is defined to be

$$Z(t^*, t) = \sum_G \prod_{v_q^*, v_q \in G} {t_q^*}^{\# v_q^*} \ {t_q}^{\# v_q} \tag{1.1}$$

where v_q^*, v_q are the vertices with q neighbours on the original and dual graph, respectively, and $\#v_q^*, \#v_q$ are the numbers of such vertices in the given graph G. Choosing $t_q^* = t_q = \delta_{q,4}$ the only allowed graphs are regular square lattices (see Fig. 1.a).

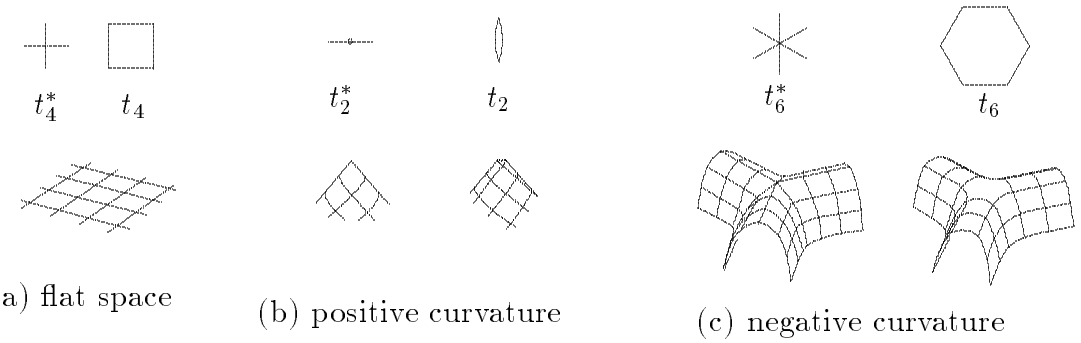

(a) flat space (b) positive curvature (c) negative curvature

Fig. 1: Flat space and curvature defects

However, it is easy to see that a regular square lattice cannot be of spherical (i.e. planar) topology. Positive curvature defects have to be added in order to be able to close the surface. Considering for the moment only even couplings, we must therefore "turn on" couplings t_2 or t_2^*, or both (see Fig. 1.b). Exactly four such defects are needed to close the square lattice. Adding more defects, then requires balancing the total curvature by also adding negative curvature defects. The simplest examples for such negative defects, corresponding to the couplings t_6 and t_6^*, are shown in Fig. 1.c. Allowing for an arbitrary number of positive and negative curvature defects we expect to generate random graphs which, at critical values of the couplings, corresponding to very big graphs dominating the sum in the partition function (1.1), allow us to reach a continuum limit lying in the universality class of pure two-dimensional quantum gravity [5] [6]. On the other hand, having "tuned away" the negative curvature couplings t_q, t_q^* with $q > 4$, no such continuum limit is possible. Then, only a small, finite number of positive curvature defects are allowed; this brings us back to the phase of essentially flat surfaces. The main physical motivation for studying the models of dually weighted graphs, then, is to understand the transition between these two very distinct phases.

In the present paper we continue to develop powerful techniques which permit us to address this physical problem. Furthermore, we will present the full and explicit solution of a non-trivial problem: the case of flat, planar graphs with an arbitrary number of positive curvature defects and a single negative curvature defect (see Fig. 2(a)) adjusted to balance the total curvature. We call the resulting lattice surfaces "almost flat planar diagrams". A typical surface of this type is shown in Fig. 2(b).

This model illustrates a non-trivial example that can be solved by the method presented in this paper. This model cannot currently be solved by standard matrix model techniques

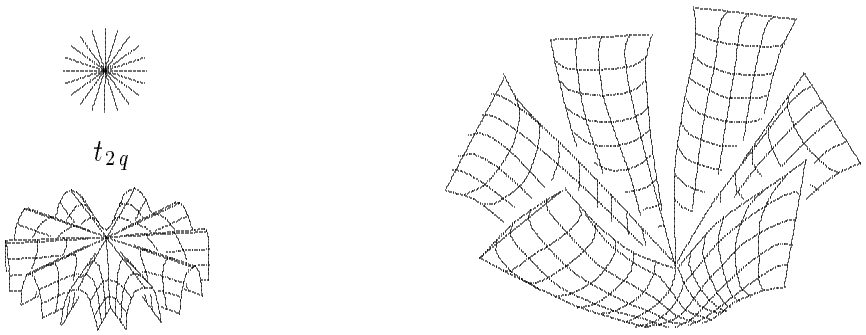

(a) (b)

Fig. 2 (a) Negative curvature defect of angle $(2-q)\pi$ and (b) a typical surface.

It should be stressed that the methods we develop here are general and could have applications going beyond the problem under investigation. Given that the model of dually weighted graphs seemed entirely inaccessible even a short while ago, we regard the present approach to be an important step in extending current large N techniques.

We will quickly recall in the next section some of the results of our previous paper [4] and precisely define the class of models we are studying. Then, in section 3, we demonstrate how to derive the large N limit of group theoretical characters. The model of almost flat planar diagrams will be solved and interpreted in section 4. The full model capturing the transition from flat to random graphs will be briefly discussed in section 5. We demonstrate how to reformulate it as a well-posed Cauchy-Riemann problem. We conclude in section 6 and present an outlook on how our approach might be put to further use in the near future. Technical details and additional illustrations are included in two appendices.

2. Review of the character expansion method for matrix models of dually weighted graphs

The partition function (1.1) for dually weighted graphs can be formulated as the following matrix model:

$$Z(t^*,t) = \int \mathcal{D}M \; e^{-\frac{N}{2}\mathrm{Tr}\; M^2 \;+\; \mathrm{Tr}\; V_B(MA)}, \tag{2.1}$$

with

$$V_B(MA) = \sum_{k=1}^{\infty} \frac{1}{k} \ \mathrm{Tr}B^k \ (MA)^k. \tag{2.2}$$

The matrices A and B are fixed, external matrices encoding the coupling constants through

$$t_q^* = \frac{1}{N} \ \mathrm{Tr} \ B^q \qquad \text{and} \qquad t_q = \frac{1}{N} \ \mathrm{Tr} \ A^q. \tag{2.3}$$

The model generalizes, for $A \neq 1$, the standard one matrix model first solved by Brézin, Itzykson, Parisi and Zuber [1]. It can no longer be solved by changing to eigenvalue variables; a reduction to N variables is nevertheless possible. An expansion of the potential into a sum over invariant group characters allows all integrations to be performed and (2.1) to be reformulated as a statistical mechanics model in "Young-tableau weight space". This reformulation should be called, after its discoverers, the "Itzykson-Di Francesco formula" [2] and reads

$$Z(t, t^*) = c \sum_{\{h^e, h^o\}} \frac{\prod_i (h_i^e - 1)!! h_i^o!!}{\prod_{i,j} (h_i^e - h_j^o)} \ \chi_{\{h\}}(A) \ \chi_{\{h\}}(B) \tag{2.4}$$

Here c is a constant that we can drop, the weights $\{h^e\}$ are a set of $N/2$ even, increasing, non-negative integers while the weights $\{h^o\}$ are $N/2$ odd, increasing, positive integers, and the sum is taken over all such sets. The characters can be defined through two equivalent formulae. The first is the Weyl formula:

$$\chi_{\{h\}}(A) = \frac{det_{(k,l)}(a_k^{h_l})}{\Delta(a)}, \tag{2.5}$$

where the a_k are the eigenvalues of the matrix A and $\Delta(a)$ is the Vandermonde determinant. The second definition makes use of Schur polynomials, $P_n(\theta)$, defined by

$$e^{\sum_{i=1}^{\infty} z^i \theta_i} = \sum_{n=0}^{\infty} z^n P_n(\theta) \quad \text{with} \quad \theta_i = \frac{1}{i} \ \mathrm{Tr}[A^i], \tag{2.6}$$

in terms of which the character is

$$\chi_{\{h\}}(A) = det_{(k,l)} \left(P_{h_k + 1 - l}(\theta) \right). \tag{2.7}$$

It was demonstrated in [4] how to take the large N limit of this expansion. In this limit, the weights $\frac{1}{N} h_i$ condense to give a smooth, stationary distribution $dh \ \rho(h)$, where $\rho(h)$ is a probability density normalized to one. For technical reasons we restrict our attention to models in which the matrices A and B are such that traces of all odd powers of A and B are zero. This means that the our random surfaces are made from vertices and

faces with even coordination numbers only. As was discussed in [4], this ensures that the support of the density $\rho(h)$ lies entirely on the real axis, and thus simplifies the solution of the problem[1]. The matrix A will satisfy this condition if we introduce an $\frac{N}{2} \times \frac{N}{2}$ matrix $\sqrt{a}$ in terms of which A and the character $\chi_{\{h\}}(A)$ are given by

$$A = \begin{bmatrix} \sqrt{a} & 0 \\ 0 & -\sqrt{a} \end{bmatrix} \quad \text{and} \quad \chi_{\{h\}}(A) = \chi_{\{\frac{h^e}{2}\}}(a)\chi_{\{\frac{h^o-1}{2}\}}(a)\ \mathrm{sgn}\Big[\prod_{i,j}(h_i^e - h_j^o)\Big], \tag{2.8}$$

We now focus our attention on three intimately related models which capture the transition from flat to random graphs.

$$\begin{aligned} &\text{I. } V_A(MA) = \sum_{k=1}^{\infty} \frac{1}{2k}\ \mathrm{Tr}[A^{2k}]\ (MA)^{2k}. \\ &\text{II. } V_{A_4}(MA) = \frac{1}{4}\ (MA)^4. \\ &\text{III. } V_A(MA_4) = \sum_{k=1}^{\infty} \frac{1}{2k}\ \mathrm{Tr}[A^{2k}]\ (MA_4)^{2k} \end{aligned} \tag{2.9}$$

Here A_4 is defined to satisfy $\mathrm{Tr}[(A_4)^k] = N\delta_{k,4}$ and A is as defined in (2.8). The first model is self-dual, i.e. vertices and faces having the same coordination number have the same weights. The second and third models are dual to each other (the lattice of one corresponds to the dual lattice of the other) and are in turn related to model I by a simple line map. That is, we place the diagonal of a square belonging to model III (or alternatively a four-vertex belonging to II) onto each propagator of model I. Thus the vertices and face centres of model I become the vertices of model III (or alternatively the faces of II). We illustrate this in Fig. 3 below[2].

---

[1] We do not want to suggest that models with odd coordination numbers cannot be treated with our methods.

[2] Note that this line-map is only valid on the sphere. The $\frac{1}{N}$ corrections of I and III will thus be different. A careful analysis shows that the spherical free energy of model I is precisely twice the free energy of models II and III (since there are two ways of choosing the diagonal of a square in III, or alternatively two ways of splitting a four-vertex of model II). Note also that this non-trivial correspondence is *predicted* from our formalism, since we indeed obtain the same $N = \infty$ equations in all three cases.

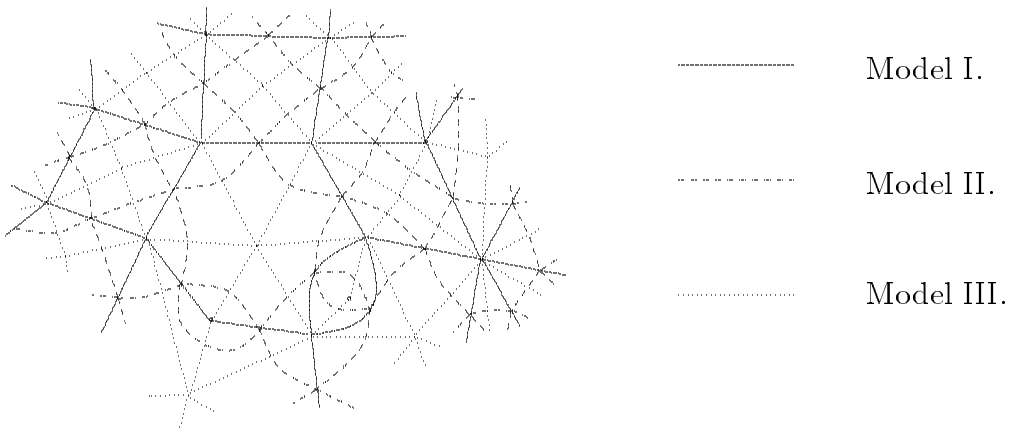

Fig. 3: Graphical relationship between models I, II and III

From this line map one can see that the expectation values in models I and III are also the same. More specifically

$$\langle \frac{1}{N} \mathrm{Tr}[(MA)^{2k}] \rangle_I = \langle \frac{1}{N} \mathrm{Tr}[(MA_4)^{2k}] \rangle_{III} \tag{2.10}$$

Notice, however, that they are not equivalent to $\langle \frac{1}{N} \mathrm{Tr}[(MA)^k] \rangle_{II}$ in model II.

We can now return to the discussion of the large N limit and write the saddlepoint equation for these three models. Looking for the stationary point in (2.4), one finds from [4], in all three cases, the following equation, valid on an interval $[b, a]$ with $0 \leq b \leq 1 \leq a$:

$$2F(h) + \int_0^a dh' \ \frac{\rho(h')}{h - h'} = -\ln h. \tag{2.11}$$

The solution requires, evidently, the knowledge of the large N limit of the variation of the characters in eq.(2.8):

$$F(h_k) = 2 \frac{\partial}{\partial h_k^e} \ \ln \ \frac{\chi_{\{\frac{h^e}{2}\}}(a)}{\Delta(h^e)}. \tag{2.12}$$

The determination of $F(h)$ is the subject of the next section. Let us also recall here the definition of the resolvent $H(h)$:

$$H(h) = \int_0^a dh' \ \frac{\rho(h')}{h - h'}. \tag{2.13}$$

In [4] we demonstrated, via a simple functional inversion, how to relate the results of the weight formalism to the resolvent $W(P) = \langle \frac{1}{N} \mathrm{Tr} \frac{1}{P-M} \rangle$ of the matrix model (2.1). In the model investigated in this paper, however, it is more natural to study the correlators $\langle \frac{1}{N} \mathrm{Tr}((MA)^{2q}) \rangle$. The results of the following section will provide a simple way to calculate such moments.

3. Large N limit of the character

In the saddle point equation (2.11) we introduced the function $F(h)$ defined in eq. (2.12) as the derivative of the logarithm of a character. This function $F(h)$ depends upon the moments of the matrix A, i.e. it contains all the information on the weights that one assigns to the faces of our discrete surfaces. In order to proceed with the solution of the saddle point equation, one would like to take the large N limit of (2.12) and express $F(h)$ in terms of $H(h)$ (which specifies the Young tableau) and the set of moments t_q of the matrix A (the weights assigned to the faces).

In [4] a contour integral formula relating $H(h)$, $F(h)$ and the set of moments t_q was derived. We recall here a single essential step of the derivation, which we will make use of shortly. We observed that

$$\mathrm{Tr}[a^q] = \sum_{k=1}^{N/2} \frac{\chi_{\{\frac{\tilde{h}^e}{2}\}}(a)}{\chi_{\{\frac{h^e}{2}\}}(a)} \quad \text{where} \quad \tilde{h}_i^e = h_i^e + 2q\delta_{i,k}, \tag{3.1}$$

and the matrix a is the $\frac{N}{2} \times \frac{N}{2}$ matrix introduced in (2.8). For notational simplicity we omit an index k on $\tilde{h}$. In the large N limit (3.1) was then reduced to a simple contour integral

$$t_{2q} = \frac{1}{q} \oint \frac{dh}{2\pi i} e^{q(H(h)+F(h))} \quad \text{where} \quad t_{2q} = \frac{2}{N}\mathrm{Tr}[a^q]. \tag{3.2}$$

Note that the definition of $F(h)$ (2.12) differs from that in the derivation in [4] since we are now restricting our attention to the case where only the even moments of the matrix A are non-zero[3].

As it stands, formula (3.2) is of little direct use. It can however be dramatically simplified as we sketch out below. We introduce a function $G(h)$ defined as

$$G(h) = e^{H(h)+F(h)}, \tag{3.3}$$

in terms of which (3.2) becomes

$$t_{2q} = \frac{1}{q} \oint \frac{dh}{2\pi i}\, G(h)^q. \tag{3.4}$$

[3] Indeed, it might be asked why we do not directly use formula (3.5) derived in section 3. of [4]. There, the contour integration relation was derived for the general case where both even and odd moments are non-zero. However, in the special case where we then set all odd moments to zero, $e^{F(h)}$ contains a cut overlapping with the cut of $e^{H(h)}$. In this case defining the contour encircling the cut of $e^{H(h)}$ is ambiguous. We have therefore rederived the result for the reduced case of only even non-zero moments. The same note of caution applies to formula (3.8) of [4].

Changing integration variables from h to G we arrive at

$$t_{2q} = \oint \frac{dG}{2\pi i G}\ h(G)\ G^q, \tag{3.5}$$

where $h(G)$ is the inverse of the equation for $G(h)$ given in (3.3), and the contour in the complex G plane encircles the origin. We now assume that there are only a finite number of non-zero couplings t_q. We obtain immediately the solution:

$$h - 1 = \sum_{q=1}^{Q} \frac{t_{2q}}{G^q}\ +\ \psi(G). \tag{3.6}$$

Here $\psi(G)$ is an as yet unknown function, analytic in the vicinity of the origin, with $\psi(0) = 0$. It is trivial to see that this satisfies (3.5). Note that, strictly speaking, we can not solve equation (3.5) for $q = 0$ since (3.4) is not defined there. The 1 on the l.h.s. of (3.6) comes from the normalization of the density $\rho(h)$ (See appendix A).

The unknown function $\psi(G)$ is not fixed by (3.4) and depends on the specific model being studied. We now give a very simple physical interpretation to this function. Let us return to the Schur polynomial definition of the character (2.7) . Differentiating eq. (2.6) with respect to θ_i we see that

$$\frac{\partial}{\partial \theta_q} P_n(\theta) = P_{n-q}(\theta) \quad \text{with} \quad \theta_q = \frac{N}{2q} t_{2q}. \tag{3.7}$$

This implies immediately that

$$\frac{2q}{N} \frac{\partial}{\partial t_{2q}} \ln\Big(\chi_{\{\frac{h^e}{2}\}}(a)\Big) = \sum_{k=1}^{N/2} \frac{\chi_{\{\frac{\tilde{h}^e}{2}\}}(a)}{\chi_{\{\frac{h^e}{2}\}}(a)} \quad \text{where} \quad \tilde{h}_i^e = h_i^e - 2q\delta_{i,k}. \tag{3.8}$$

From (2.1), (2.4) and (2.8), we see that the left hand side of this equation is equivalent to differentiating the logarithm of the original matrix integral (2.1) with respect to t_{2q}. In terms of the dual to this matrix integral (in which the weights t_{2q} assigned to the faces are now the weights of the vertices) this is equivalent to differentiating the coupling constants of the dual potential. So, denoting the dual matrix by $\tilde{M}$, the left hand side of eq. (3.8) is equivalent to the expectation value $\langle \mathrm{Tr}(\tilde{M}B)^{2q} \rangle$. Now, comparing the right hand side of (3.8) to equations (3.1) and (3.2), we see that we have the following relation in the large N limit,

$$\langle \frac{1}{N} \mathrm{Tr}(\tilde{M}B)^{2q} \rangle = \oint \frac{dG}{2\pi i G}\ h(G)\ G^{-q}, \tag{3.9}$$

$G(h)$ being defined by (3.3). It is now simple to follow identical arguments to those used to simplify (3.4) to (3.6) to arrive at

$$h - 1 = \sum_{q=1}^{Q} \frac{t_q}{G^q} + \sum_{q=1}^{\infty} \langle \frac{1}{N} \mathrm{Tr}\ (\tilde{M}B)^{2q} \rangle\ G^q. \tag{3.10}$$

Given $G(h)$, we have, after a functional inversion, the correlators of the dual model.

To find $G(h)$ we have to connect eq. (3.10) with the saddle point equation (2.11). From (2.13) we obtain

$$H(h) = \ln \frac{h}{h-b} + \tilde{H}(h) \quad \text{with} \quad \tilde{H}(h) = \int_b^a dh' \frac{\rho(h')}{h - h'}, \tag{3.11}$$

where the first term on the right is the contribution from the flat part of the density, i.e. the empty part of the Young tableau. The integral from b to a is the contribution from the "excited" part of the density, i.e. the non-empty part of the Young tableau. Noting, from the definition of $G(h)$ (3.3), that $\ln G(h) = H(h) + F(h)$, we replace the integral of (3.11) by the contour integral

$$\tilde{H}(h) = \oint \frac{dh'}{2\pi i}\ \frac{\ln G(h')}{h - h'} \tag{3.12}$$

where the contour encircles the $[b, a]$ part of the cut of $H(h)$. The discontinuity across this cut is precisely $\pm i\pi\rho(h)$. Note also that $F(h)$ has – at least for some range of the couplings – no cut on the interval $[b, a]$. If we now change the variables of integration from h to G, as previously, and shrink the contour in the complex G plane catching poles on the way (see appendix A), we arrive at the following simple relationship between equation (3.6) and $H(h)$:

$$e^{H(h)} = \frac{(-1)^{(Q-1)} h}{t_Q} \prod_{q=1}^{Q} G_q(h). \tag{3.13}$$

Some words of explanation are in order to clarify the meaning of this equation. Inverting eq. (3.6) leads to a multi-sheeted function $G(h)$. The general picture is illustrated in Fig. 4. One of the sheets is the physical sheet and has two cuts, one corresponding to $e^{H(h)}$, the other to $e^{F(h)}$; we label this sheet $G_1(h)$. The sheets $G_2(h), \ldots, G_Q(h)$ are all the sheets connected to $G_1(h)$ by the cut of $e^{F(h)}$; there are exactly Q of these sheets, where Q is the maximum inverse power of G in (3.10).

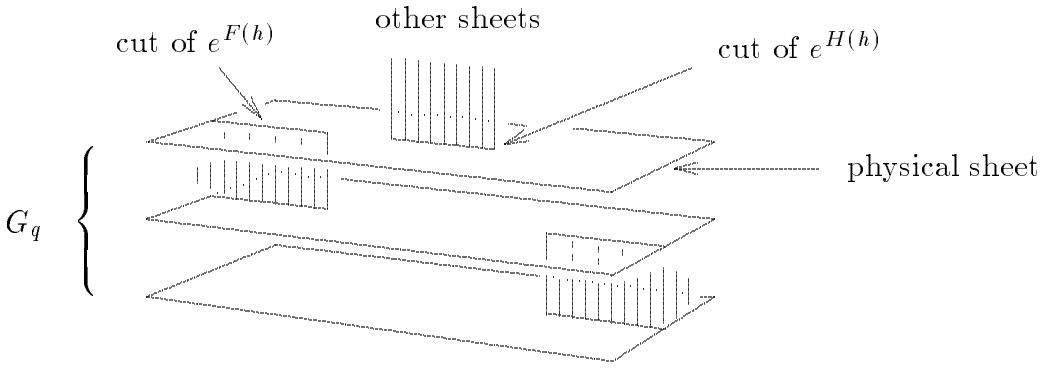

Fig. 4: Analytic structure of $G(h)$

In appendix B several examples are presented to illustrate explicitly this general analytic structure.

Equation (3.13) together with (3.10) contains sufficient information to find the logarithmic derivative of the character. These two equations represent a well-defined Cauchy-Riemann problem for $F(h)$ which can be explicitly solved. We will present the solution elsewhere.

4. Almost flat planar diagrams

We now have all the tools necessary to reduce our model of dually weighted graphs to a well defined Cauchy-Riemann problem. In this section we will analyse the case in which only positive curvature defects are allowed on the surface, arbitrary amounts of negative curvature being introduced at a single point. This is done by studying the particular case $t_q = t_2\delta_{q,2} + t_4\delta_{q,4}$, which generates the flat patches (see Fig. 1(a)) and the positive defects (see Fig. 1(b)). The correlators (2.10) then correspond to the insertion of a single defect of curvature $(2-k)\,\pi$ (see also Fig. 2). They will be extracted using eq.(3.10), after explicit calculation of the function $h(G)$.

From the analysis of the large N limit of the character in the previous section, we know that the product in (3.13) contains only two sheets $G_q(h)$ (see Fig. 4). We label the physical sheet $G_1(h)$ and the sheet connected to it by the cut of $e^{F(h)}$, $G_2(h)$. Taking the logarithm of equation (3.13), we summarize the information extracted from the large N limit of the character by

$$F_1(h) + F_2(h) + H(h) = -\ln(-\frac{h}{t_4}), \tag{4.1}$$

where $\ln G_i(h) = F_i(h) + H(h)$. The two sheets $G_1(h)$ and $G_2(h)$ are glued together by the square root cut coming from $F(h)$. The combination $F_1(h) + F_2(h)$, evaluated on the cut of $F(h)$, is twice the constant part of $F(h)$ on the cut (the discontinuous part of $F(h)$ is of opposite sign on $F_1(h)$ and $F_2(h)$ and is therefore canceled). We thus have the two equations

$$\begin{aligned} 2\not{F}(h) + H(h) &= -\ln(-\frac{h}{t_4}) \\ 2F(h) + \not{H}(h) &= -\ln h, \end{aligned} \tag{4.2}$$

the first coming from the large N limit of the character (3.13) and the second being the saddlepoint equation (2.11). These two equations tell us about the behaviour of the function $2F(h) + H(h)$ on the cuts of $F(h)$ and $H(h)$ respectively. We have introduced the notation $\not{F}(h)$ to denote the real part on the cut of $F(h)$, and similarly for $\not{H}(h)$. The principal part integral in (2.11) is thus denoted in (4.2) by $\not{H}(h)$.

Our object now is to reconstruct the analytic function $2F(h)+H(h)$ from its behaviour on its cuts. To do this we have to understand the complete structure of cuts. First we notice from (3.6) that $G(h)$ is non zero everywhere in the complex h plane except at infinity. The combination $F(h) + H(h)$ thus has no logarithmic cut point except for the one which starts from $h = b$. This corresponds to the end of the flat part of the density $\rho(h)$. We introduce two functions $\tilde{F}(h)$ and $\tilde{H}(h)$ defined by

$$F(h) = \tilde{F}(h) - \ln h \quad \text{and} \quad H(h) = \tilde{H}(h) + \ln \frac{h}{h-b}, \tag{4.3}$$

in terms of which (4.2) becomes

$$\begin{aligned} 2\not{\tilde{F}}(h) + \tilde{H}(h) &= \ln\bigl(-t_4(h-b)\bigr) \\ 2\tilde{F}(h) + \not{\tilde{H}}(h) &= \ln(h-b). \end{aligned} \tag{4.4}$$

These two equations define the behaviour of $2\tilde{F}(h) + \tilde{H}(h)$ on all of its cuts. By standard methods we now generate the full analytic function $2\tilde{F}(h)+\tilde{H}(h)$. We introduce three cut points, a, b and c whose values are fixed by boundary conditions (the points a and b define the cut of $\tilde{H}(h)$ and c defines the starting point of the cut of $\tilde{F}(h)$ which goes from c to $-\infty$) and generate the full analytic function by performing the contour integral

$$\begin{aligned} 2\tilde{F}(h) + \tilde{H}(h) = \sqrt{(h-c)(h-b)(h-a)}\Biggl[&\oint_{C_H} \frac{ds}{2\pi i} \frac{\ln(s-b)}{(h-s)\sqrt{(s-c)(s-b)(s-a)}} \\ &+ \oint_{C_F} \frac{ds}{2\pi i} \frac{\ln\bigl(-t_4(s-b)\bigr)}{(h-s)\sqrt{(s-c)(s-b)(s-a)}}\Biggr]. \end{aligned} \tag{4.5}$$

The contours C_H and C_F are illustrated in Fig. 5(a). The slanted zigzag line corresponds to the cut of $\ln(h-b)$. Expanding the contours, catching poles on the way and using the fact that logarithmic cuts have a discontinuity of $\pm i\pi$, we arrive at

$$2F(h)+H(h) = \ln\frac{t_4}{h} + \sqrt{(h-c)(h-b)(h-a)}\Big[\int_c^b \frac{ds}{(h-s)}\frac{1}{\sqrt{(s-c)(s-b)(s-a)}} + \int_b^a \frac{ds}{(h-s)}\frac{\frac{1}{\pi i}\ln t_4}{\sqrt{(s-c)(s-b)(s-a)}}\Big]. \tag{4.6}$$

Fig. 5(b) clarifies the sign convention for $\sqrt{(h-c)(h-b)(h-a)}$ on the real axis above and below the cuts. Note that, for the cuts of $1/\sqrt{(h-c)(h-b)(h-a)}$ the signs on the cuts are inverted compared to Fig. 5(b), i.e. $+i \leftrightarrow -i$. The integrals in (4.6) are defined to be along the upper side.

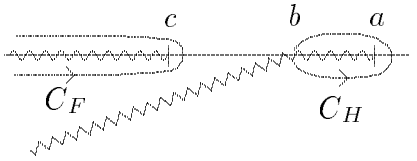

(a) Contours for (4.5)

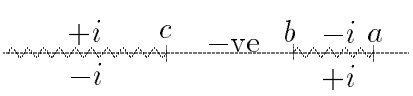

(b) Sign convention for $\sqrt{(h-c)(h-b)(h-a)}$

Fig. 5: Contours and sign conventions for (4.5) and (4.6)

To fix the constants a, b and c, we expand (4.6) for large h and compare the resulting power series expansion to that obtained from inverting (3.6):

$$2F(h)+H(h) = \ln\frac{t_4}{h} + \frac{1}{\sqrt{h}}\frac{t_2}{\sqrt{t_4}} \quad + \quad \mathcal{O}\big(\frac{1}{h\sqrt{h}}\big). \tag{4.7}$$

The terms of $\mathcal{O}\big(\frac{1}{h\sqrt{h}}\big)$ depend on the as yet unknown function $\psi(G)$. Expanding (4.6) for large h and comparing to (4.7) we find the two boundary conditions

$$t_4 = q = e^{-\pi\frac{K'}{K}} \quad \text{and} \quad \frac{t_2}{\sqrt{t_4}} = \frac{\pi}{K}\sqrt{a-c}, \tag{4.8}$$

with K and K' complete elliptic integrals of the first kind, defined in terms of their respective moduli k and $k' = \sqrt{1-k^2}$ through

$$k = \sqrt{\frac{a-b}{a-c}}. \tag{4.9}$$

The first condition fixes k and hence the ratio of the distances separating the cut points, and the second condition fixes $a-c$, i.e. the scale. The condition needed to fix the position of the cut points along the real axis is provided by the condition that the density must be normalized to one.

We now perform the integrals in (4.6) and, after using the first boundary condition and an identity between elliptic functions[4], we obtain

$$2F(h)+H(h) = -\ln h - \frac{i\pi}{K}\mathrm{sn}^{-1}\Big(\sqrt{\frac{a-h}{a-b}},k\Big), \tag{4.10}$$

where $\mathrm{sn}^{-1}(z,k)$ is the inverse Jacobi elliptic function. Using the saddle point equation $2F(h)+\not{H}(h) = -\ln h$ and the fact that the resolvent for the Young tableau can be written as $H(h) = \not{H}(h) \mp i\pi\rho(h)$, we can immediately write down the expression for the density of Young tableau boxes as

$$\rho(h) = \frac{1}{K}\mathrm{sn}^{-1}\Big(\sqrt{\frac{a-h}{a-b}},k\Big). \tag{4.11}$$

The Jacobi elliptic function $\mathrm{sn}(z,k)$ is a generalisation of $\sin(z)$ with quarter period K. In fact, in the limit $k\to 0$, which corresponds to $t_4\to 0$, the expression for the density becomes precisely $(2/\pi)\sin^{-1}(\sqrt{(a-h)/(a-b)})$.

Integrating $\rho(h)$ from b to a and equating the answer to $1-b$ to ensure that the density is normalized to 1 (the flat portion from 0 to b gives a contribution b), gives the final boundary condition

$$a = 1+\frac{t_2^2}{\pi^2 t_4}(K^2-EK), \tag{4.12}$$

where E is the complete elliptic integral of the second kind.

From the expression for the density we now generate the full Young tableau resolvent, $H(h)$, in the standard way and obtain following expression:

$$\begin{aligned} H(h) =& \frac{h}{h-b}+\int_b^a dh'\ \frac{\rho(h')}{h-h'} \\ =& \ln h - \frac{i\pi}{K}\mathrm{sn}^{-1}\sqrt{\frac{a-h}{a-b}} + 2\ln\left(\frac{\theta_4\Big(\frac{\pi}{2K}\mathrm{sn}^{-1}\sqrt{\frac{a-h}{a-b}}\Big)}{q^{1/4}\big[(a-c)(a-b)\big]^{1/4}\theta_4(0)}\right). \end{aligned} \tag{4.13}$$

Using the above expression for $H(h)$, the eq. (4.10) for $2F(h)+H(h)$ and the quasi-periodicity of theta functions, we can write the expression for $G(h)$,

$$G(h) = -\frac{1}{D}\theta_4\Big(\frac{\pi}{2K}\mathrm{sn}^{-1}\sqrt{\frac{a-h}{a-b}}+\frac{i\pi K'}{K}\Big) \tag{4.14}$$

[4] For this and many other relations between Jacobi's elliptic functions and theta functions useful for performing the calculations of this section see e.g. [8],[9].

and its inverse

$$h = a - \frac{q^{3/2}}{G^2}\Big[\frac{\theta_1\big[\theta_4^{-1}(-GD)\big]}{\theta_4(0)}\Big]^2, \tag{4.15}$$

where the constant D is given by

$$D = \frac{t_2 K\sqrt{k}\ \theta_4(0)}{\pi q^{5/4}} = \frac{t_2\theta_1'(0)}{2q^{5/4}}. \tag{4.16}$$

To simplify (4.15) we have used the definition of the Jacobi elliptic function in terms of theta functions. In view of eq.(3.10), we see that we have now explicitly calculated the generating function for the correlators for models I and III.

We will now expand eq.(4.15) and read off the correlators as the coefficients of the positive powers of G. Notice that (4.15) is a multivalued function since the function $\theta_4(z)$ is periodic as z is varied in the real direction and quasiperiodic in the imaginary direction. We must thus choose the correct zero of the $\theta_4(z)$ function about which to expand. The physical sheet corresponds to expanding about the zero $z = \frac{i\pi K'}{K}$. Using the definition of the Jacobi elliptic function $\mathrm{sn}(u)$ in terms of theta functions and shifting the arguments of the theta functions using their quasi-periodicity, we rewrite (4.15) as the pair of equations

$$h = a + \frac{q}{G^2}\Big(e^{iz}\frac{\theta_4(z)}{\theta_4(0)}\Big)^2 \quad \text{with } z \text{ the solution of} \quad \frac{t_2 G}{2q} = ie^{iz}\frac{\theta_1(z)}{\theta_1'(0)}. \tag{4.17}$$

Expanding this for small G we find that the first three terms give (as expected from (3.10)) $h = \frac{q}{G^2} + \frac{t_2}{G} + 1 + \mathcal{O}(G)$. Expanding three orders further, permits us (using (3.10)) to read off the first three moments of model III (which are also the moments of model I):

$$\begin{aligned}
\Big\langle\ \frac{1}{N}\ \mathrm{Tr}\ [(MA_4)^2]\ \Big\rangle_{III} =& \frac{t_2^3}{24q^2}(1+f_3)\\
\Big\langle\ \frac{1}{N}\ \mathrm{Tr}\ [(MA_4)^4]\ \Big\rangle_{III} =& \frac{t_2^4}{192q^3}\big(-8(1+f_3)+3f_2^2-4f_2f_3+f_4\big)\\
\Big\langle\ \frac{1}{N}\ \mathrm{Tr}\ [(MA_4)^6]\ \Big\rangle_{III} =& \frac{t_2^5}{1920q^4}\big(81+90f_3-30f_2^2+40f_2f_3+10f_3^2-10f_4-f_5\big).
\end{aligned} \tag{4.18}$$

where for convenience we have defined

$$\begin{aligned}
f_2 =& \frac{\theta_4''(0)}{\theta_4(0)} &=& \frac{4}{\pi^2}(K^2-EK)\\
f_4 =& \frac{\theta_4''''(0)}{\theta_4(0)} &=& \frac{16K^2}{\pi^4}\big((3-2k^2)K^2-6EK+3E^2\big)\\
f_3 =& \frac{\theta_1'''(0)}{\theta_1'(0)} &=& \frac{4}{\pi^2}\big((2-k^2)K^2-3EK\big)\\
f_5 =& \frac{\theta_1''''(0)}{\theta_1'(0)} &=& \frac{16K^2}{\pi^4}\big((6-6k^2+k^4)K^2-10(2-k^2)EK+15E^2\big).
\end{aligned} \tag{4.19}$$

and have then expressed these derivatives as combinations of the complete elliptic integrals K, E and their modulus k.

We can now give a simple physical interpretation of these moments. The first two are directly related to the free energy $\mathcal{F}(t_2, t_4)$. The latter is defined as the sum over all possible surfaces with the topology of a sphere that can be constructed out of flat space and positive curvature defects. It is impossible to put a flat surface onto the sphere, so positive curvature defects are needed to close the surface. Since the defects in this model have a deficit angle of π it takes precisely four of them to close the surface into a sphere. The surfaces are in the form of a cylinder with both ends flattened. The four t_2 defects sit at the corners. Below we illustrate the free energy for model III:

$$\mathcal{F}(t_2, t_4) = \sum$$ 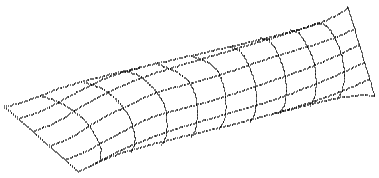 (4.20)

Note that the flattened ends can have an angle of twist between them. The four t_2 defects correspond to vertices $\frac{t_2}{2}$ Tr $[(MA_4)^2]$, and all other vertices (with four legs) correspond to the vertex $\frac{t_4}{4}$ Tr $[(MA_4)^4]$. We see that the first two moments can be written in terms of the free energy $\mathcal{F}(t_2, t_4)$ as

$$\begin{aligned} \langle\ \frac{1}{N}\ \mathrm{Tr}\ [(MA_4)^2]\ \rangle_{III} &= 2\frac{\partial}{\partial t_2}\mathcal{F}(t_2, t_4) \\ \langle\ \frac{1}{N}\ \mathrm{Tr}\ [(MA_4)^4]\ \rangle_{III} &= 4\frac{\partial}{\partial t_4}\mathcal{F}(t_2, t_4). \end{aligned} \tag{4.21}$$

We thus read off the free energy

$$\mathcal{F}(t_2, t_4) = \frac{t_2^4}{192 q^2}(1 + f_3). \tag{4.22}$$

Using (4.19), the identity $\frac{\partial}{\partial q} = \frac{2K^2 k k'^2}{\pi^2 q}\frac{\partial}{\partial k}$, along with standard identies for differentiating complete elliptic integrals with respect to the modulus k, it is trivial to verify that the moment $\langle\ \frac{1}{N}\ \mathrm{Tr}\ [(MA_4)^4]\ \rangle_{III}$ given in (4.18) is indeed four times the derivative of the free energy with respect to $t_4 = q$.

Using the definition of f_3 in terms of derivatives of the first theta function, $\theta_1(z)$, along with the standard definition of the theta function as an infinite product, allows us to write the free energy as

$$\mathcal{F}(t_2, t_4) = \frac{-t_2^4}{8}\frac{\partial}{\partial q^2}\ln\Big[\prod_{n=1}^{\infty}(1 - q^{2n})\Big] = \sum$$ 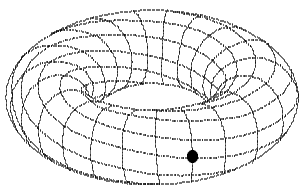 (4.23)

In this form we recognize the argument of the logarithm to be the partition function for the torus. The derivative operator acts to mark a single point. We have thus found, as illustrated in equation (4.23), that the free energy can be written as the free energy for a marked torus. Below we illustrate the connection between a marked torus and the flattened cylinder diagrammatically.

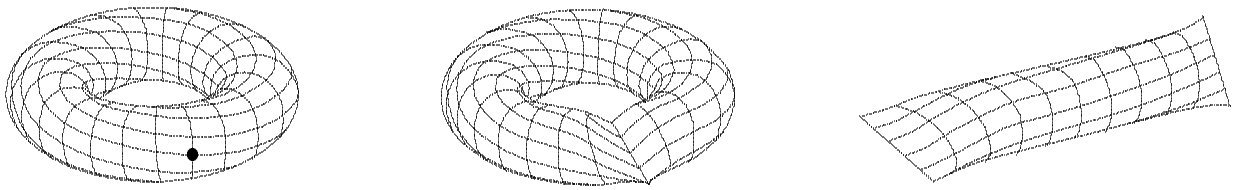

Fig. 6 Diagrammatic connection between marked torus and flattened cylinder.

Starting from the mark on the twisted torus, flatten the torus across its width (this defines a point on the opposite side), then cut along the flattening and open out the crimped torus into a cylinder with flattened ends. The two points at either end of the flattening on the torus become the four t_2 defects of the flattened cylinder.

Higher order moments correspond to inserting a single negative curvature defect. The lowest order defect of this type is the insertion of negative curvature of deficit angle $-\pi$ introduced by the vertex $\mathrm{Tr}[(MA_4)^6]$ (see Fig. 1(c) and eq. (4.18)).

As a final check of our solution, we expand $\langle\ \frac{1}{N}\ \mathrm{Tr}\ [(MA_4)^6]\ \rangle_{III}$ in powers of q (this can be done directly from the expression for the moment in terms of theta functions (4.18)):

$$\langle\ \frac{1}{N}\ \mathrm{Tr}\ [(MA_4)^6]\ \rangle_{III} = t_2^5\ (\ 9q^2\ +\ 27q^4\ +\ 81q^6\ +\ \ldots). \tag{4.24}$$

It is easy to verify that this correctly counts the number of diagrams.

Further moments can be calculated by expanding (4.17) to higher order. They can always be written as sums of products of complete elliptic integrals.

We now look for a continuum limit in which the size of graphs tends to infinity. One can see that the critical point, at which the size of the graphs diverges, is at $q = 1$. Note, however, that (since the critical q is 1), in stark contrast to two-dimensional quantum gravity [5] [6], the leading behaviour for the growth of diagrams is *not* exponential but merely power-like. To extract the power, notice that the product $\prod_{n=1}^{\infty}(1-q^{2n})$ in (4.23) can be written in terms of the η function as $q^{-1/12}\eta(i\tau)$ where $q = e^{-\pi\tau}$. Making use of the

modular invariance of the $\eta(\tau)$ function under the the modular transformation $\tau \to 1/\tau$, we extract

$$\mathcal{F}(t_2, 1-\mu) \sim \frac{\pi^2 t_2^4}{192} \frac{1}{\mu^2}, \tag{4.25}$$

where we have defined a "continuum cosmological constant" μ through $q = 1 - \mu$ i.e. $\mu = \pi\tau + \mathcal{O}(\tau^2)$. We thus see, changing from fixed cosmological constant to fixed area by Laplace transform, that the number of graphs grows as a linear power of the area. Employing the conventions of quantum gravity [5] [6], this would formally correspond to a "string susceptibility" $\gamma_{str} = 4$.

We can easily understand this result by performing the calculation directly in the continuum limit. We thus integrate over cylinders of all possible lengths t and circumferences s weighted with a factor s (corresponding to the modular twist between the two flattened ends) and a delta function for the area so as to count the number of surfaces of a given area A. We thus perform the following integral:

$$\mathcal{F} \sim \int_0^\infty dt\ ds\ s\ \delta(ts - A) = A \int_0^\infty \frac{dt}{t^2}. \tag{4.26}$$

We see immediately a linear dependence on the area A, but also a divergently large contribution coming from small t. The most important contribution comes from the cylinders which are infinitely short and thus have the maximum amount of entropy coming from the modular twist.

It is interesting now to investigate the behaviour of the correlators in the large area ($q \to 1$) limit. Quite generally, for matrix models the correlators correspond to surfaces with a boundary of length proportional to the power of the correlator, and one seeks a continuum scaling limit for very long boundaries. The correlators $\langle\ \frac{1}{N}\ \mathrm{Tr}\ [(MA_4)^{2n}]\ \rangle$ in the present model, however, introduce point-like negative curvature and we cannot look for a scaling limit involving long boundaries[5]. Nevertheless we can find the limiting behaviour of these negative curvature insertions in the limit of large area.

Using the modular transformation $\tau \to 1/\tau$ (with $q = e^{-\pi\tau}$) for the formula (4.15), we can also extract a scaling limit for the generating function for the moments. Specifically, for the theta functions $\theta_1(z)$ and $\theta_4(z)$, we find that the dominant contributions are

$$\begin{aligned} \theta_4(z) &= \frac{1}{\sqrt{\tau}} e^{-\frac{\tau}{\pi} y^2} 2q'^{1/4} \big(\cosh y + \mathcal{O}(q'^2)\big) \\ \theta_1(z) &= \frac{1}{\sqrt{\tau}} e^{-\frac{\tau}{\pi} y^2} 2q'^{1/4} \big(\sinh y + \mathcal{O}(q'^2)\big), \end{aligned} \tag{4.27}$$

[5] In principle, it is possible to study boundaries of arbitrary length by taking correlators of $\langle\ \frac{1}{N}\ \mathrm{Tr}\ [(MA_4^2)^{2n}]\ \rangle$, which correspond to a boundary in the form of the end of a cylinder. Technically, however, we do not at present have the means to calculate such quantities.

where $y = z/\tau$ and $q' = e^{-\frac{\pi}{\tau}}$. Holding y fixed as a parameter of order 1, we take the limit as $\tau \to 0$ (corresponding to $q \to 1$) and work to the first two orders in τ. Remembering that $q = 1 - \pi\tau + \ldots$, the constants D and a to the first two orders in τ are given by

$$D = t_2 \frac{1}{\tau^{3/2}} q'^{1/4} \big(1 + \frac{5}{4}\pi\tau\big) \quad \text{and} \quad a = 1 + t_2^2 \Big[\frac{1}{4\tau^2} - \big(\frac{1}{2\pi} - \frac{\pi}{4}\big)\frac{1}{\tau}\Big], \tag{4.28}$$

We can now define a natural rescaled parameter $x = \frac{Gt_2}{2\tau}$ and perform the inversion of the theta function to the first two orders in τ to find the generating function for the correlators. The lowest order term gives the contribution $\frac{q}{G^2}$ in (3.10) and also a part that cancels with $a - 1$. The next order gives the contribution $\frac{t_2}{G}$ along with the generating function which we read off as:

$$\sum_{n=1}^{\infty} \langle\ \frac{1}{N}\ \mathrm{Tr}\ [(MA_4)^{2n}]\ \rangle G^n = \frac{t_2}{\tau}\Big[\frac{\sin^{-1} x - x}{2x^2} + \frac{(\sin^{-1} x)^2 - x^2}{2\pi x^2}\Big] \quad \text{with} \quad x = \frac{Gt_2}{2\tau}. \tag{4.29}$$

This has a simple square root singularity at the point $x = 1$. The series expansions for $\sin^{-1} x$ and $(\sin^{-1}(x))^2$ then give us the dominant contribution to the correlators in the large area limit:

$$\langle\ \frac{1}{N}\ \mathrm{Tr}\ [(MA_4)^{2n}]\ \rangle \simeq \frac{C_n t_2^{n+2}}{\mu^{n+1}} \quad \text{with} \quad \begin{cases} C_{2n} = \frac{\pi^{2n}(n!)^2}{2\ (2n+1)!\ (n+1)} \\ C_{2n+1} = \frac{\pi^{2n+2}(2n+2)!}{2^{4n+4}((n+1)!)^2(2n+3)}, \end{cases} \tag{4.30}$$

where we have again introduced the parameter μ defined by $q = 1 - \mu$ i.e. $\mu = \pi\tau + \mathcal{O}(\tau^2)$. The number of surfaces of fixed area A for a correlator $\langle\ \frac{1}{N}\ \mathrm{Tr}\ [(MA_4)^{2n}]\ \rangle$ is thus seen to be of the order of A^n, with entropy coming from modular twists analogous to those for the free energy. The rather curious structure of the considered surfaces is thus evident - they consist of cylindrical "fingers" growing out from the negative curvature defect (see Fig. 2(b)). The square root singularity at $x = 1$ means that there is a tree-like growth of the number of ways to attach the fingers to their base at the negative defect. As in the case of the free energy, modular integrations cause a filamentary structure of very long cylinders to dominate in the large area limit.

5. The onset of quantum gravity: Adding negative curvature defects

The introduction of arbitrary numbers of negative defects, specifically t_6, alongside the components t_4, t_4^* and positive curvature defects, t_2, gives us a model in which we can tune away the curvature fluctuations of two-dimensional quantum gravity. The large N limit of the character in section 3 allows us to understand the analytic structure of

the solution and thus reduce the model to a well defined Cauchy-Riemann problem. The function $G(h)$ now consists of two sheets below the physical sheet (see Fig. 4). An extra sheet which we label $G_3(h)$ is now attached to the sheet $G_2(h)$ of the previous section by a square root cut. We thus have the following two equations

$$\begin{aligned} 2F(h) + \not{H}(h) &= -\ln h \\ F_1(h) + F_2(h) + F_3(h) + 2H(h) &= -\ln(\frac{h}{t_6}) \end{aligned} \quad . \tag{5.1}$$

The first is the saddle point equation (2.11). The second comes from the logarithm of eq. (3.13), where we define, as before, $F_i(h)$ by $\ln G_i(h) = H(h) + F_i(h)$. Along with the boundary conditions provided by the coefficients of the negative powers of G in (3.10), the system of equations (5.1) completely determines the solution to this problem.

6. Conclusions and outlook

In the present work we have demonstrated that our technique of character expansions for large N matrix models may be successfully applied to the study of a novel, up to now inaccessible phase of almost regular planar diagrams. This required determining – quite generally – the large N limit of Weyl characters through the functional equation (3.13). Specializing to almost flat graphs, we have then found the exact generating function (3.10), (4.15) of planar square lattices endowed with a single negative curvature insertion balanced by a number of positive defects.

We feel that our observations could trigger the investigation of many new phenomena in two-dimensional physics and the combinatorial theory of planar graphs. However, most urgent is the understanding of the crossover phenomenon from the phase of almost flat two-dimensional space to the phase of two-dimensional quantum gravity. It requires the careful analysis of the well-posed Cauchy-Riemann problem of the last section. This investigation is pending. Aside its obvious mathematical interest, the solution of this problem could help to solve the hitherto inaccessible problem of R^2 quantum gravity in two dimensions.

In addition to the even lattices considered in this paper, our methods allow the study of the "melting" of more general regular, or almost regular, lattices; e.g. triangular lattices.

It is well known that there are many intriguing relations between integrable two-dimensional models on regular lattices and dynamical planar random lattices. It is tempting to try to unify the two classes of models, a project one might term GUT_2. Our work should be considered a first attempt into this direction, even though it must be noted that further methods will have to be developed in order to successfully treat matter coupled to dually weighted graphs.

Some of the results presented above could be interpreted as insights into the structure of the group $SU(\infty)$ (see section 3 on the large N limit of Weyl characters.). Further insights into this direction might prove very useful for the treatment of higher dimensional matrix models, e.g. the principal chiral field, discrete string theories in physical dimensions and, one hopes, QCD.

Acknowledgements

We would like to thank E. Brézin and I. Kostov for useful discussions.

Appendix A. Derivation of the inversion formula

We start by proving that the constant coefficient in (3.6) is equal to 1 (the normalization of the density). To correctly normalize the density, $\rho(h)$, we have to ensure that

$$1 - b = \int_b^a dh \rho(h). \tag{A.1}$$

Using the fact that $\ln G(h) = H(h) + F(h)$, we replace the integral by the contour integral

$$1 - b = \oint_{C_H} \frac{dh}{2\pi i} \ln G(h), \tag{A.2}$$

with the contour C_h encircling the $[b, a]$ part of the cut of $H(h)$, as shown in Fig. 7. The zig-zag line corresponds to the logarithmic cut starting at $h = b$. Note that this is not a closed contour since at b there is a discontinuity across the cut of $\pm i\pi$. Evaluating $G(h)$ around this contour we see that its argument goes from $+i\pi$ at $h = b$ (below the cut) all the way around to $-i\pi$ at $h = b$ (above the cut). We now change integration variables from h to G, with (in light of the comment above) the contour C_G in the complex G plane encircling the origin (see Fig. 7):

$$1 - b = -\oint_{C_G} \frac{dG}{2\pi i} h'(G) \ln G(h) = -\oint_{C_G} \frac{dG}{2\pi i} \Big[\frac{\partial}{\partial G}(h(G) \ln G) - \frac{h(G)}{G} \Big], \tag{A.3}$$

where $h(G)$ is defined through (3.6). The contour starts and finishes on either side of the cut generated by $\ln G$ illustrated in Fig.7 by a zig-zag line. The total derivative term picks up the discontinuity across the cut giving $-b$. The final term, which picks up the constant coefficient of $h(G)$, is thus equal to 1.

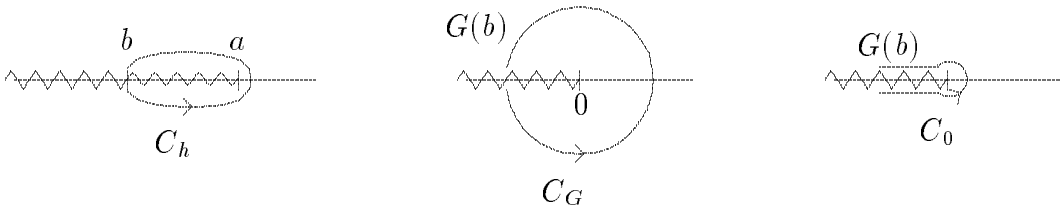

Fig. 7: Definition of contours C_h in the complex h plane and C_G and C_0 in the complex G plane.

We now complete the derivation of (3.13). As discussed in section 3. we start by generating $\tilde{H}(h)$ (related to the full resolvent by $H(h) = \tilde{H}(h) + \ln \frac{h}{h-b}$) from the contour integral

$$\tilde{H}(h) = \oint_{C_h} \frac{dh_1}{2\pi i} \frac{\ln G(h_1)}{h - h_1}. \tag{A.4}$$

Changing integration variables from h to G, as above, this can be written as

$$\tilde{H}(h) = -\oint_{C_G} \frac{dG}{2\pi i} \ln G \frac{h'(G)}{h - h(G)}, \tag{A.5}$$

where $h(G)$ is defined through (3.6) and $h'(G)$ is the derivative with respect to G.

We now simplify this contour integral by evaluating it for large h. Knowing the solution in any neighbourhood of h means that, by analytic continuation, we know it everywhere. For large enough h, we see from (3.6) that the contour in (A.5) will encircle precisely Q zeros of $h(G)$, the zeros corresponding to the inverse powers of G. If we shrink the contour in (A.5) so that the contour hugs either side of the cut (see Fig. 7, contour C_0) we pick up these Q poles:

$$\tilde{H}(h) = \sum_{q=1}^{Q} \ln G_q(h) - \oint_{C_0} \frac{dG}{2\pi i} \ln G \frac{h'(G)}{h - h(G)}. \tag{A.6}$$

The remaining contour integral is relatively easy to evaluate provided careful attention is paid to the contribution coming from encircling the origin. The net result is that the contour C_0 contributes $\ln\big((-1)^{Q-1} t_{2Q}\big)$ from encircling the origin and $\ln(h-b)$ from the discontinuity across the end points of the contour. Putting these results together and making use of the relationship between $H(h)$ and $\tilde{H}(h)$ we arrive at (3.13).

Appendix B. Analytic structure of $G(h)$

As is discussed in Appendix A, the sheets $G_q(h)$ in the product of (3.13) are the physical sheet and all the sheets attached to the physical sheet by the cut of $e^{H(h)}$. To clarify this we provide some simple examples.

B.1. Example 1. $V_B(MA) = 0$

In this simplest case it is immediate from eq.(3.10) (since $B = 0$ and thus $\psi(G) = 0$) that

$$h - 1 = \sum_{q=1}^{Q} \frac{t_{2q}}{G^q}. \tag{B.1}$$

This is a polynomial equation of degree Q. $G(h)$ will thus be a multivalued analytic function with Q sheets. The different sheets are connected by square root cuts, represented in Fig. 8 below by the vertical walls.

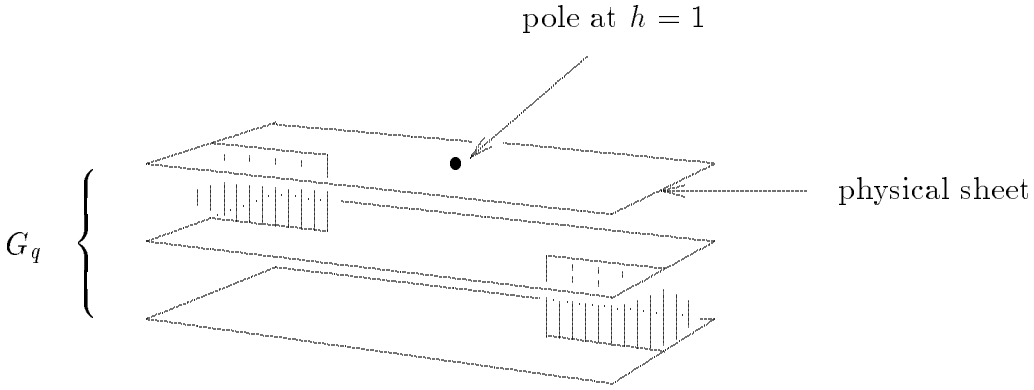

Fig. 8: Analytic structure of $G(h)$ for $V_B(MA) = 0$

Note that cube roots and higher order roots are just special cases of the above structure. For example, a cube root in the diagram above is generated when the two square root cut points touch.

The $G_q(h)$ that enter the product in (3.13) are precisely all the solutions, i.e. all the sheets. It then follows that

$$e^{H(h)} = \frac{h}{h-1}, \tag{B.2}$$

which corresponds to a completely flat density $\rho(h) = 1$ with support $[0, 1]$.

It is seen from equation (B.1) that at $h = 1$, $G(h)$ becomes infinite on one of its sheets, so there is a pole at $h = 1$ on what we call the physical sheet. For $\psi(G)$ non zero, the positive powers of G "soften" this pole and stretch it into a cut. The cut corresponds to exciting boxes in the Young tableau. The next example illustrates this.

B.2. Example 2. $V_B(MA) = MA$

Here $B = A_1$. It follows from eq.(3.10) and a simple diagrammatic inspection that

$$h - 1 = \sum_{q=1}^{Q} \frac{t_{2q}}{G^q} \quad + \quad G \tag{B.3}$$

This increases the degree of the polynomial by one from the previous example, introducing an extra sheet. The pole that was at $h = 1$ has now opened into a cut (the cut of $e^{H(h)}$) connected to this extra sheet (see Fig. 9).

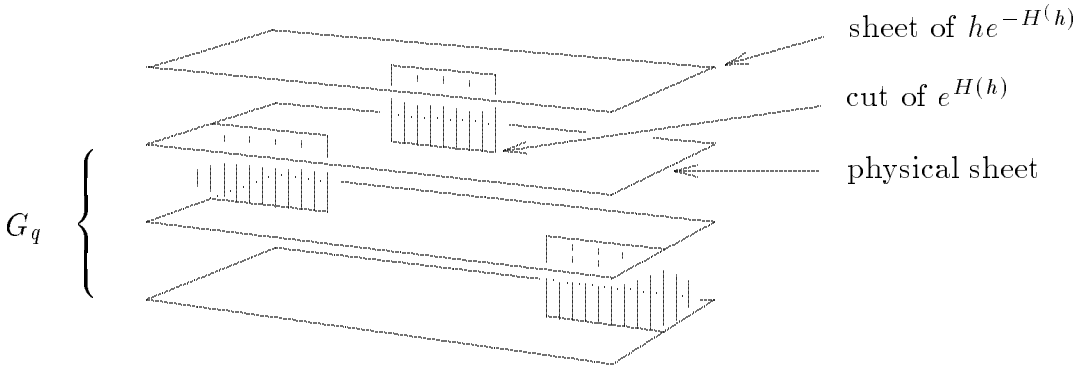

Fig. 9: Analytic structure of $G(h)$ for $V_B(MA) = MA$

The $G_q(h)$ that go into the product of eq.(3.13) are the physical sheet and all the sheets below. We thus obtain

$$e^{H(h)} = \frac{h}{G^-(h)}, \tag{B.4}$$

where $G^-(h)$ is the topmost sheet.

B.3. Example 3. $V_B(MA) = (MA)^2$

By inspecting the moments of the dual model, we obtain

$$h - 1 = \sum_{q=1}^{Q} t_{2q} \ (\frac{1}{G^q} + G^q). \tag{B.5}$$

The sheet structure is still polynomial, but now, due to the symmetry $G \to G^{-1}$ of equation (B.5), the top sheets are the mirror image inverses of the bottom sheets.

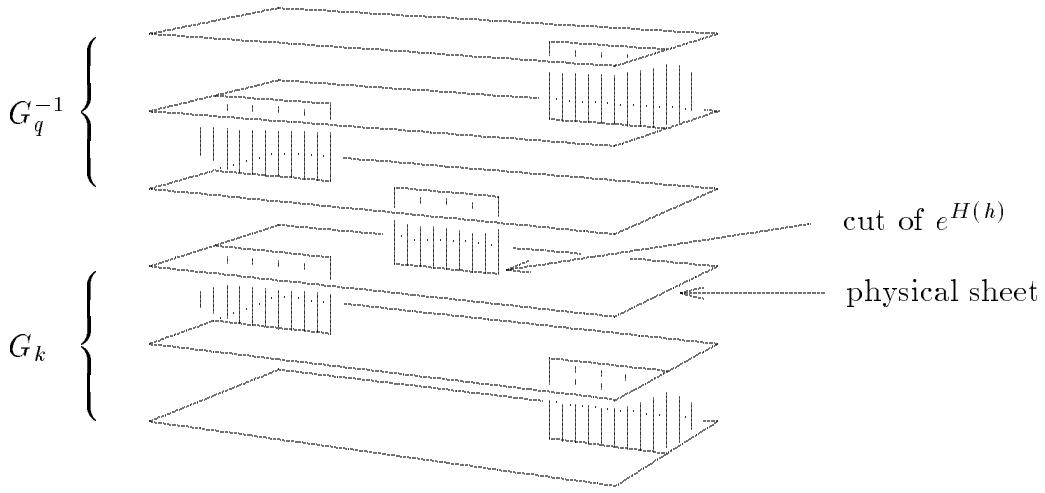

Fig. 10: Analytic structure of $G(h)$ for $V_B(MA) = (MA)^2$

Again, what was a pole at h=1 has opened into a cut connecting the physical sheet to the mirror image inverses of the bottom sheets.

The above three examples clarify the meaning of equations (3.10) and (3.13). A simple functional inversion developed in [4] allows us to relate $H(h)$ to the resolvent, $\langle \mathrm{Tr}\big[\frac{1}{P-M}\big]\rangle$, of the matrix model. To verify the methods of section 3, we have directly calculated the matrix resolvent of these models using loop equations and simple diagrammatic arguments.

References

[1] E. Brézin, C. Itzykson, G. Parisi & J.-B. Zuber, Commun. Math. Phys. 59 (1978), 35.

[2] P. Di Francesco & C. Itzykson, Ann. Inst. Henri. Poincaré Vol. 59, no. 2 (1993) 117.

[3] C. Itzykson & J.-B. Zuber, J. Math. Phys. 21(3) (1980) 411.

[4] V.A. Kazakov, M. Staudacher & T. Wynter, École Normale preprint LPTENS-95/9, accepted for publication in Commun. Math. Phys.

[5] F. David, Nucl. Phys. B257 (1985) 45.

[6] V.A. Kazakov, Phys. Lett. B150 (1985) 282.

[7] J. Fröhlich, in: Lecture Notes in Physics, Vol. 216, Springer, Berlin, 1985;
J. Ambjørn, B. Durhuus and J. Fröhlich, Nucl. Phys. B257[FS14](1985) 433.

[8] P.F. Byrd & M.D. Friedman, "Handbook of Elliptic Integrals for Engineers and Physicists", Springer, Berlin, 1954.

[9] D.F. Lawden, "Elliptic Functions and Applications", Springer, New York, 1989.